



The function of hydrophobic cathodic backing layers for high energy passive direct methanol fuel cell

Jing Zhang, Ligang Feng, Weiwei Cai, Changpeng Liu, Wei Xing*

State Key Laboratory of Electro-analytical Chemistry, Laboratory of Advanced Power Sources, Changchun Institute of Applied Chemistry, Graduate School of the Chinese Academy of Sciences, 5625 Renmin Street, Changchun, Jilin 130022, PR China

ARTICLE INFO

Article history:

Received 31 March 2011

Received in revised form 10 July 2011

Accepted 11 July 2011

Available online 20 July 2011

Keywords:

Back-flow

Passive direct methanol fuel cell

Hydrophobic cathodic backing layer

Energy density

ABSTRACT

Homemade wet-proofing carbon papers with back-flow effect were applied as backing layers in the cathode of passive air-breathing direct methanol fuel cell (DMFC) fed by pure methanol. With the increase of polytetrafluoroethylene (PTFE) content, the carbon papers exhibited different water transport resistance and generated different back-flow effects. Moreover, PTFE-treated carbon papers were observed by scanning electronic microscope (SEM) to investigate the function of the cross-linked microstructure. Maximum energy density (438 WhL^{-1}) of the improved pure methanol DMFC was obtained by using carbon paper with 40 wt.% PTFE content as the cathodic backing layer. This value was 6 times larger than that of the conventional DMFC fed by 2 M methanol solution.

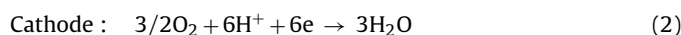
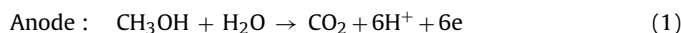
© 2011 Elsevier B.V. All rights reserved.

1. Introduction

Direct methanol fuel cells (DMFCs) are regarded as promising electrochemical system for directly converting the chemical energy of methanol and oxygen into electric energy in a wide range, especially for portable power sources [1,2]. Although extensive efforts have been made to develop passive DMFC technology over the past decades, the overall cell performance has not reached the expected level for most electronic devices [3]. One of the issues is the short runtime and low energy density for the passive DMFC caused by using low methanol concentration. Passive DMFC fed by high concentration methanol or the pure methanol has been identified as one of the most promising candidates for the future development of portable power sources [4–7].

In our previous work [8], a novel passive DMFC structure was proposed with pervaporation membrane to control the methanol transport when the fuel cell was fed by pure methanol (DMFC-P). The results showed that the discharge time of the proposed DMFC-P at 100 mA was increased about 6 times as compared with that of the conventional DMFC fed by 3 M methanol solution, and the proposed passive DMFC-P was worthy of further study. However, the passive DMFC-P still confronted the problem of water shortage

during long-term operation. As we know, water is necessary for the anodic reaction which can be seen from the following equations.



From the reactions, water is consumed in the anodic reaction, but more water is produced in the cathodic reaction. Therefore, it is a reasonable and possible way to utilize the water produced in the cathodic side for passive DMFC-P. Many efforts have been made to fabricate a water back-flow electrode to make use of the water produced in the cathode [9–14]. For example, Faghri et al. [11] developed an additional thick gas diffusion layers on the cathodic side to increase the hydraulic pressure which forced water back to the anodic side of the cell. Zhao et al. [13] summarized the mass transport modes of reactants transport for the DMFCs fed by concentrated methanol and the effects of water backflow from the cathode to anode were further explained.

Although some reports have been done to the water back-flow in the DMFC, the technology was usually combined with a special kind of fuel cell structure. Based on our previous proposed passive DMFC-P structure, in the present study, different contents of hydrophilic ionomer (5 wt.% Nafion solution) and hydrophobic additive polytetrafluoroethylene (PTFE) were added to each layer of membrane electrode assembly (MEA) to build hydrophobicity gradient for dynamic back-flow. Through the treatment of polytetrafluoroethylene (PTFE), the carbon papers with different hydrophobicity were prepared as cathodic backing layers (CBLs).

* Corresponding author. Tel.: +86 431 85262223; fax: +86 431 85685653.
E-mail address: xingwei@ciac.jl.cn (W. Xing).

And the effects of the hydrophobic structure on the performance of the DMFCs fed by pure methanol were systematically evaluated.

2. Experimental

2.1. Fabrication of membrane electrode assembly

Before the MEA fabrication, the required carbon papers (TGP-H-030, Toray) with different hydrophobicity were prepared by the treatment of PTFE. First, carbon papers were accurately weighed and then immersed in PTFE emulsion (40 wt.%, DuPont, USA) for different times which depended on the final hydrophobicity of the carbon paper. During the impregnation course, it was necessary to stir the emulsion continuously and brush the surface of carbon papers several times to keep PTFE spread uniformly on the surface. Second, the carbon papers were heat treated in the muffle furnace at 340 °C for 30 min. The PTFE particles on the surface were melted to liquid and then infiltrated into the interspaces of carbon fibers above melting point of 327 °C. Finally, carbon papers were weighed again after the heat treatment to calculate the actual amount of PTFE. The impregnation-sinter courses of carbon papers were repeated until reaching the expected PTFE content. A series of hydrophobic carbon papers with PTFE loading from 10 wt.% to 50 wt.% were prepared in this way.

The hydrophobic properties of carbon papers are evaluated using the contact angle test by sessile drop method [15,16]. In this method, droplet of water is placed on the surface of carbon paper and the contact angle is measured by special instrument (DSA100, KRÜSS Company, Germany). Micro-scale morphology of the carbon paper was observed by scanning electron microscope (SEM, FEI, Netherlands). The samples were cleaned with water and ethanol solution, and cut into tiny pieces in liquid nitrogen before observation.

The above treated carbon papers with different hydrophobicity were used as cathodic backing layer (CBL). Then the microporous layers (MPL) composed of carbon black (Vulcan XC-72) and PTFE were spread onto the carbon papers for anode and cathode to form the gas diffusion layers (GDL) [17,18]. The carbon loading for the MPL in cathode and anode was 2 mg cm⁻², and the PTFE content for the diffusion layers was 20 wt.% and 10 wt.% in cathode and anode, respectively. Finally, the GDL was dried at room temperature and sintered in air at 340 °C for half an hour to distribute the PTFE homogeneously throughout the MPL [19–21].

The catalyst ink was made by dispersing the catalyst (PtRu black for anode and Pt black for cathode, Johnson Matthey Co.) with a mixture of 5 wt.% Nafion ionomer solution (DuPont, USA), isopropanol, and de-ionized (DI) water. The volume ratio of isopropanol and DI water was 50:1. The suspension was stirred in ultrasonic cleaner for 45 min and then sprayed on the GDL with an ultrasonic syringe to form catalyst layer [19]. The Pt black loading was 8.0 mg cm⁻² and the Nafion content was 10 wt.% in the cathode catalyst layer. The PtRu black loading was 8.0 mg cm⁻² and the Nafion content was 20 wt.% in the anodic catalyst layer. A Nafion 117 membrane (DuPont, Co.) was used as the polymer electrolyte membrane. The pretreatment process of the membrane included boiling the membrane in 5 vol.% H₂O₂, washing in DI water, boiling in 0.5 M H₂SO₄ and washing in DI water for 1 h in turn [22]. Finally, the MEA was fabricated by sandwiching the Nafion membrane between the anode and the cathode, and was hot-pressed at 135 °C and 5 MPa for 3 min. The prepared MEAs were immersed in DI water overnight for activation and humidification. The apparent area of the MEA was 3.0 cm × 3.0 cm.

Ultimately, the proposed back-flow MEA structure (shown in Fig. 1) can be divided into the following seven layers: Nafion membrane, highly hydrophobic backing layer, hydrophobic MPL,

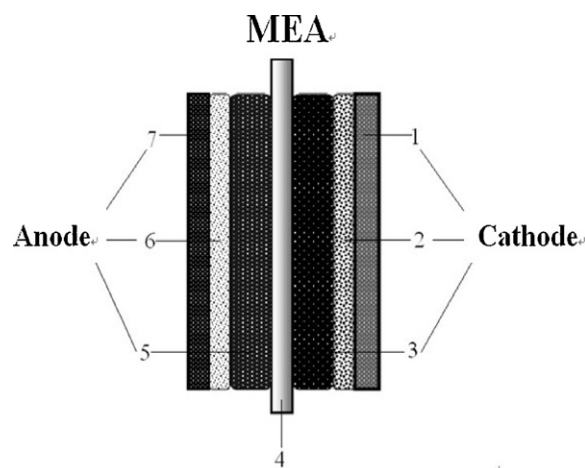


Fig. 1. Structure of improved back-flow membrane electrode assembly. (1) Hydrophobic backing layer with above 30 wt.% PTFE, (2) less hydrophobic MPL with 20 wt.% PTFE, (3) hydrophilic catalyst layer with 10 wt.% Nafion, (4) Nafion 117 membrane, (5) more hydrophilic catalyst layer with 20 wt.% Nafion, (6) less hydrophobic MPL with 10 wt.% PTFE, and (7) less hydrophobic backing layer with 10 wt.% PTFE.

hydrophilic catalyst layer for the cathode and more hydrophilic catalyst layer, less hydrophobic MPL, less hydrophobic backing layer for the anode. Due to the hydrophobicity gradient between different layers, the water produced in the cathode was prevented from diffusing to air through backing layer and could be spontaneously driven back from cathodic catalyst layer to anodic catalyst layer by the strengthened hydraulic force [9,12].

2.2. Fuel cell performance measurements

A homemade single passive DMFC fed by pure methanol was fabricated according to our previous work [8]. In brief, the fuel reservoir was divided into two tanks: a pure methanol tank (12 mL) and a low methanol concentration cushion tank (5 mL). Before the discharge test, 3 mL DI water was injected into the cushion tank for initial humidification. The pervaporation membrane was fixed between the two tanks to control the methanol transport. The MEA was positioned between two current collectors, which were made of gilded stainless steel meshes. A pair of 0.5 mm thick silicon rubber gaskets was used to prevent fuel leakage from the cell. Cathodic backing layers with PTFE content of 10 wt.%, 20 wt.%, 30 wt.%, 40 wt.% and 50 wt.% were marked as CBL10, CBL20, CBL30, CBL40 and CBL50, respectively. The polarization curves of the single fuel cell were measured with a Fuel Cell Test System (Arbin Instruments Co.) under ambient conditions. The discharge curves of voltage vs. time were also tested at a constant current.

3. Results and discussion

From the viewpoint of water management in DMFC, the water flux between anode and cathode is determined by electro-osmotic drag, diffusion and hydraulic permeation [9]. Electro-osmotic drag in the cell is caused by hydrogen protons pulling water through the Nafion membrane during discharge course. Diffusion of water takes place due to species and concentration gradients. And hydraulic permeation is caused by pressure gradient of water across the membrane. For DMFC fed by dilute solution, the three forces are prone to drive water from anode to cathode. However, for passive DMFC fed by pure methanol, diffusion and hydraulic permeation are possible to benefit the water back-flow from cathode to anode. Furthermore, the hydraulic permeation can be accelerated by modifying the hydrophobicity of cathode and hydrophilicity of anode.

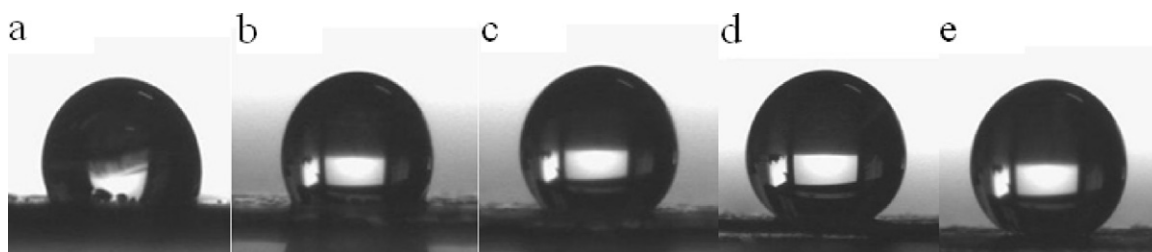


Fig. 2. Contact angle images of carbon papers with the PTFE loading of (a) 0 wt.%, (b) 10 wt.%, (c) 20 wt.%, (d) 30 wt.% and (e) 40 wt.%.

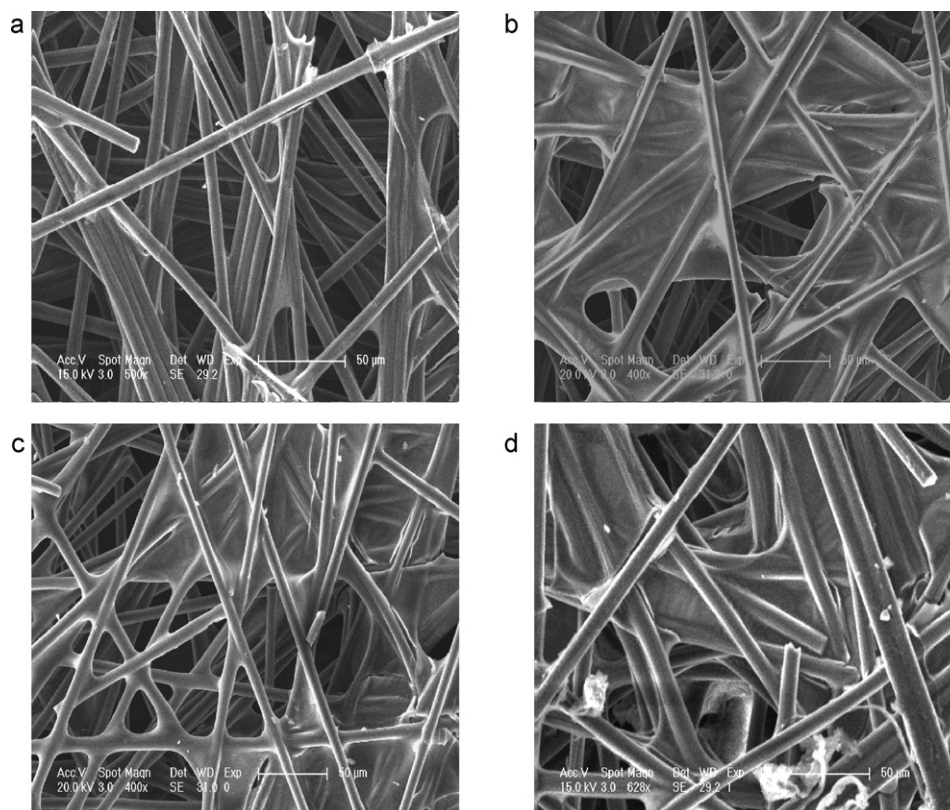


Fig. 3. SEM images of hydrophobic carbon papers (a) 0 wt.% PTFE, (b) 20 wt.% PTFE, (c) 30 wt.% PTFE and (d) 40 wt.% PTFE.

So it is necessary to investigate the surface wetting properties of carbon papers.

Surface contact angle values and the corresponding PTFE content of the carbon papers are presented in Table 1. From the results it can be concluded that the untreated carbon paper with 0 wt.% PTFE already exhibited hydrophobicity and the contact angle was about 101° , which was consistent with the previous report [23]. When the carbon paper was impregnated with PTFE, the contact angles rose with the increase of PTFE content rapidly and displayed higher hydrophobicity, but above the content of 20 wt.% the increasing tendency was quite gentle instead of linear growth. The contact angle stopped increasing at the PTFE content of 40 wt.% (154°), which was regarded as the upper limit of the PTFE content in the carbon paper, and the surface of carbon paper was almost completely overlaid by PTFE [24]. There was no significant increase of contact angles when the PTFE content was above 50 wt.% (151°).

Table 1
Contact angle values of carbon papers with different PTFE contents.

PTFE content	0 wt%	10 wt.%	20 wt.%	30 wt.%	40 wt.%	50 wt.%
Contact angle	101°	128°	142°	149°	154°	151°

In order to evaluate the hydrophobic effect of the cathodic carbon paper after PTFE-treatment, the water droplet images during contact angle test are shown in Fig. 2. The images manifest the effects of surface hydrophobicity on water transport: water droplet was slippery on the surface of carbon paper for high PTFE content (above 30 wt.% PTFE) and the contact area was so small that the water could not permeate the surface and internal micropores of carbon paper easily. As the barrier to hold up cathodic water, carbon paper with large water transport resistance was needed to prevent the water from diffusing to air. By contrast, liquid water spreads stantly on the surface of carbon paper for relatively low PTFE content (below 20 wt.% PTFE). It is certain that the less hydrophobic carbon paper with larger contact area enjoyed more chances for the water penetration, namely, less water transport resistance. Liquid water produced in the cathodic reaction could easily pass through the less hydrophobic carbon paper and evaporate to the atmosphere, which reduced the total amount of back flow. Since the hydraulic force had the ability to control the water content and flow direction between the adjacent layers by different hydrophobicity [9], the hydrophobic treatment of the carbon papers was necessary.

Morphology of carbon paper in micro scale was investigated by SEM (shown in Fig. 3). It can be seen that the pores among the

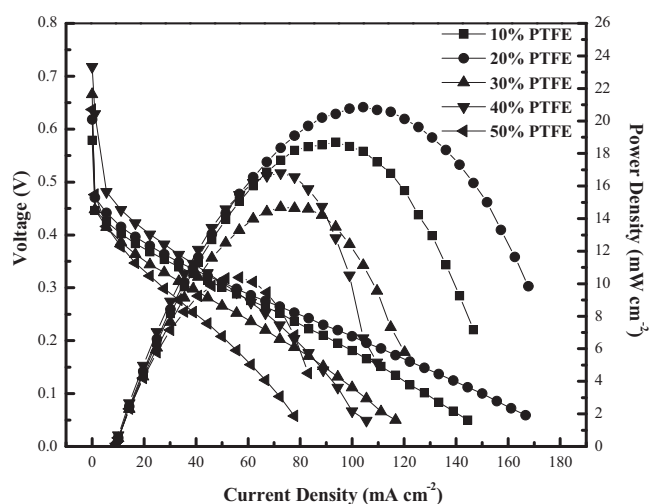


Fig. 4. Polarization curves of passive air-breathing DMFC fed by 2 M methanol.

carbon fibers distributed from several microns to tens of microns and the sintered PTFE polymers exhibited a spatial extension and adhered firmly to the porous structure of carbon fibers. With the increase of PTFE content, the polymer networks became thicker and more adhesive. Previous literatures [14,25–27] suggested that this hydrophobic PTFE networks play an important role for water transport and provide micro-channels for air-breathing on the cathodic side. Since the size of micro pores among the PTFE networks is large enough for oxygen molecule transport, the increase of PTFE content has low influence on the oxygen diffusion in the PTFE networks. Meanwhile, due to the high hydrophobicity and thick microstructure, cathodic backing layers with high PTFE loading can generate efficient water blocking effect, which lays the foundation of the following back-flow as expected. So the adoption of PTFE-treated carbon paper as CBL was the primary requirement for back-flow effect, which was indispensable for our proposed DMFC system fed by pure methanol.

In order to know the actual effect of PTFE-treated carbon papers on mass transport of DMFC, the different hydrophobic carbon papers were used and tested in a conventional passive DMFC with 2 M methanol solution (Fig. 4). It can be seen from Fig. 4 that the cell performance is closely associated with the hydrophobicity of CBL. When the PTFE content in the CBL was 10 wt.%, the maximum power density of the DMFC was 19 mW cm^{-2} . With 20 wt.% PTFE CBL, the DMFC can obtain maximum power density up to 23 mW cm^{-2} , which was the highest one among the five CBLs. Cell performance decreased with the increasing of PTFE content above 20 wt.% and the maximum power density of DMFC finally reduced to 10 mW cm^{-2} for 50 wt.% CBL. It is confirmed in the previous work [23] that the addition of PTFE brings a great increase of electric resistance to carbon paper and the resistance displays a gentle increase above 10 wt.% PTFE. In general, the optimal performance of passive DMFC is determined by two key factors: mass transport and electric conductivity. It is certain that the increase of insulated polymer PTFE takes the responsibility for the performance decline. Meanwhile, the remove of cathodic water is difficult due to the high hydrophobicity and leads to serious flooding [9,10,19] at high current density. The flooding is commonly caused by the accumulation of excessive water, which blocks the micro-channel for oxygen diffusion. However, when adopting low hydrophobic carbon papers such as 10 wt.% in the cathode, the remove of water is still difficult due to the sticky property of the less hydrophobic micro-channel. The cathodic flooding limits the oxygen transport in cathode and finally brings negative influence on the cell performance during the operation. Therefore, a balance between water transport and elec-

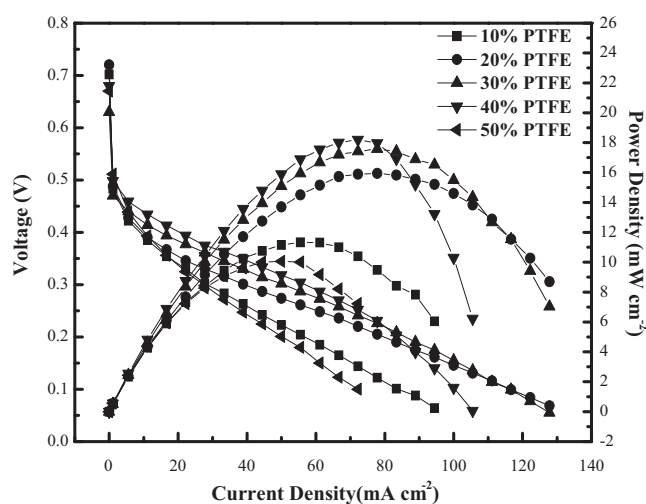


Fig. 5. Polarization curves of DMFC-P with different CBLs.

tric resistance needs to be built by controlling the PTFE content of cathodic carbon paper to achieve optimal cell performance.

In the following step, the DMFC-P with the above MEA was tested to evaluate the actual function of hydrophobic carbon paper. The polarization curves are shown in Fig. 5. It can be seen that the power density of the five cells showed an overall decline, compared to the DMFCs fed by solution. The highest power density belonged to the DMFC-P with CBL30, which was lower than 20 mW cm^{-2} . Performances of DMFCs-P with CBL30 and CBL40 were similar and higher than that of the DMFCs-P with CBL20 and CBL10. And DMFC-P with CBL50 was still the lowest one due to the large electric resistance. The performance decline of DMFC-P could be attributed to the lack of fuel in the anodic catalyst layer. The anodic catalyst layer of conventional DMFC fed by dilute solution is always immersed in solution and the mass transport of methanol in the aqueous medium is very fast. Thus the methanol concentrations keep nearly the same in different parts until fuel exhaustion. But for the DMFC-P, the concentration of methanol solution in cushion tank is controlled by methanol transport through pervaporation membrane. The estimate of the methanol concentration in the cushion compartment can be found in our previous work [8]. Because the methanol was slowly transported to the anodic catalyst layer, it would limit the DMFC-P performances. The weakness was not evident at low current density but became the vital factor at high current, when the anodic reaction demanded a large amount of methanol. Without sufficient fuel to attend anodic reaction under such condition, the maximum output power of DMFC-P was decreased as compared with the DMFC fed by methanol solution. It can be concluded that the DMFC-P is not suitable to work at high current density.

However, it is not proper to evaluate the performance merely according to the polarization curve. For many portable electrical devices, the starting and working current is not very high (often below 20 mA cm^{-2}). So the detailed function of hydrophobic CBL for DMFC-P was further studied through long-term discharge test at a relatively lower current range. In our work, the discharge experiments at 100 mA and 200 mA were carried out for further investigation. The voltages of the cells were recorded every 2 h and the $V-t$ curves are presented in Fig. 6(a) and (b) for 100 mA and 200 mA, respectively. It can be seen from Fig. 6(a) that the five curves exhibited different trends after a few hours. In the initial 10 h, the DMFC-P experienced a sudden voltage decline and a slow recovery from the lowest value due to the accumulated heat [6–8], which increased the catalyst activity. The cell voltages of DMFCs-P with CBL10 and CBL20 could reach 0.40 V after 10 h. However, the

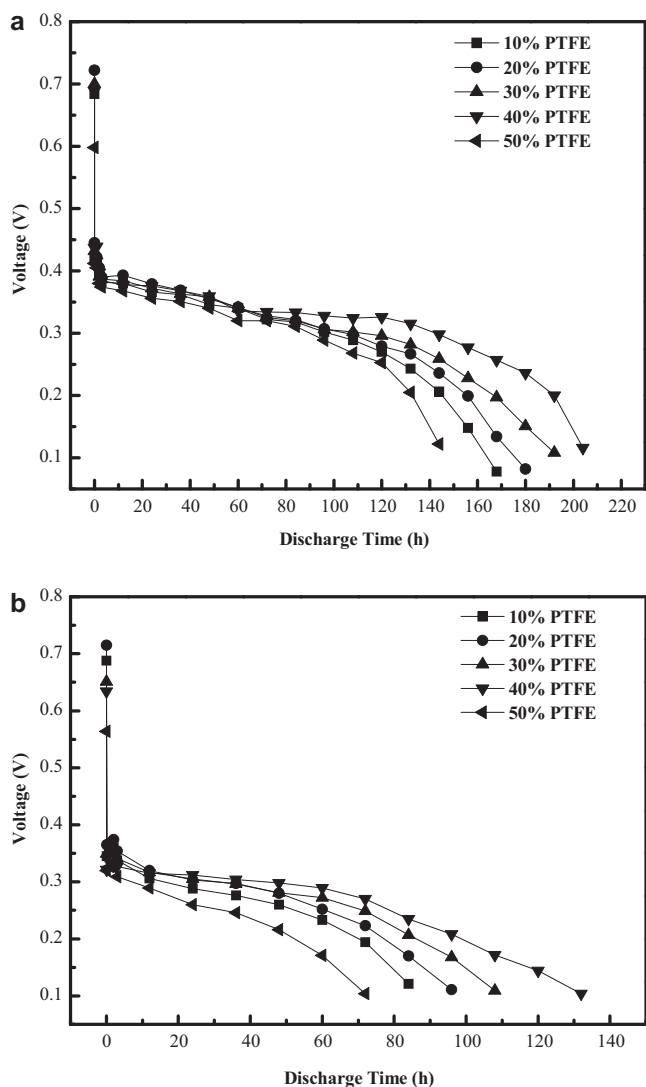


Fig. 6. Long-term discharge curves of DMFC-P with different CBLs at (a) 100 mA and (b) 200 mA.

maximum voltages of DMFCs-P with CBL30 and CBL40 could only reach 0.38 V due to the larger resistance of PTFE. After 10 h, the voltages for all DMFCs-P with different CBLs fluctuated between 0.35 V and 0.38 V, and then stabilized in the next 50 h. From 60 h to 100 h, the cell voltages dropped slowly with time due to the accumulation of poisonous side products. In this period, the voltage decline of DMFCs-P with low hydrophobic CBL was larger than those of DMFCs-P with highly hydrophobic CBL. At 100 h, the cell voltage of DMFC-P with CBL10 turned lower than that with CBL30 and CBL40. In the following time, DMFC-P voltage with CBL10 and CBL20 decreased rapidly, while that with CBL30 and CBL40 still maintained a relatively steady value. It is confirmed from the volume of methanol in reservoir that insufficient methanol took the responsibility for performance decline after discharge. Passive air-breathing DMFC-P with CBL40 had the longest operation time over 200 h.

Fig. 6(b) shows the $V-t$ curves of the DMFCs-P operated at 200 mA. With the doubled speed of fuel consumption, duration time was significantly shortened. It is presented that DMFC-P with CBL40 exhibited the best performance among the five cells. And the cells with CBL10 and CBL50 still showed weak performance. Fig. 6 indicates that DMFC-P with hydrophobic CBL40 exhibited the most effective utilization of methanol and the best

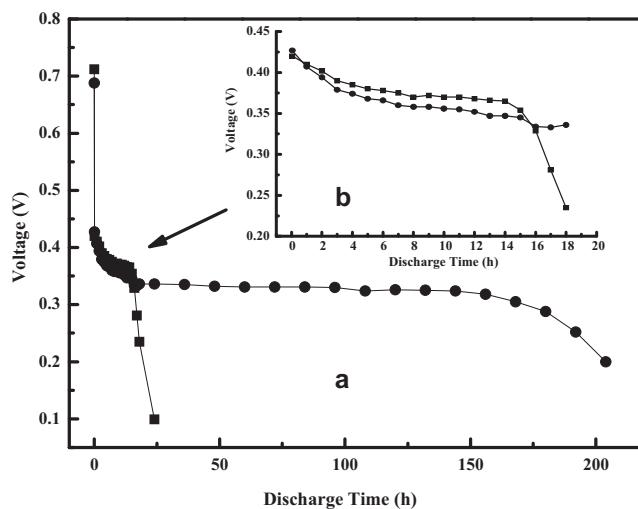


Fig. 7. Discharge curves of (●) DMFC-P (■) DMFC fed by 2 M methanol solution at 100 mA during (a) the 200 h operation and (b) the initial 20 h operation.

stabilization of voltage during long-term operation. The voltage stability during continuous operation can be explained in terms of water management in the cathode side. Based on the conventional theory and experiences, more PTFE in the CBL would increase electric resistance and hinder the water remove from the cathode, which produced negative influence on electric conductivity and mass transport in DMFC-P. However, the negative effects of high hydrophobicity were overcome by some positive factors under the continuous discharge operation with pure methanol. The reason can be explained as follows: firstly, blocking effect of highly hydrophobic CBL provided a basis of internal flow of generated water instead of diffusing to air. Then the accumulated water in the cathode was driven to flow back due to the different wettability as well as concentration gradient from cathode to anode. The water back from cathode dilutes the pure methanol in anodic catalyst layer. Meanwhile, the back-flow water could bring proportional amount of methanol with it. This reduced the net methanol crossover for the DMFC-P. Ultimately the above factors enhanced the practical efficiency of DMFC-P. In concert with the low hydrophilic catalyst layer in the anode, DMFC-P with CBL40 achieved the optimal combination of excellent back-flow effect and tolerable electric resistance. In contrast, DMFC duration with CBL10, CBL20 and CBL30 were not satisfactory due to weak back-flow effect. In the two operations at 100 mA and 200 mA the CBL50 brought deterioration to DMFC-P, which was attributed to the large electric resistance.

In order to clearly show the advantage of DMFC-P, the DMFC-P with the optimal CBL of 40 wt.% PTFE content and the DMFC fed by 2 M methanol solution with optimal CBL of 20 wt.% PTFE content were compared under the same discharge condition (100 mA) and the $V-t$ curves are shown in Fig. 7. The voltage fluctuation of the two cells in the initial 20 h is also inserted in Fig. 7. It is confirmed that the DMFC-P exhibited a relatively stable performance during 100 h operation, and then decreased gently. By contrast, the voltage of DMFC fed by 2 M solution was a little higher than DMFC-P in the initial 20 h but only stabilized for 10 h followed by a drastic decrease. The reasons for the performance decline over time are complex and several limiting factors such as species poisoning, methanol supply and water management are discussed in the above results. Because of the same reactants and the catalysts employed in the fuel cells, the performances decline affected by the poisoning species should be similar in the two kinds of fuel cells. From the curves of Fig. 7, it was evident that the significant decline of cell performance in the later stage should be mainly affected by the amount of fuel

(methanol and water) supply. When the methanol concentration was lower than the fuel required for normal anodic reaction, the performance was reduced. Since the DMFC-P fed by pure methanol can provide more methanol than the DMFC fed by solution in the same volume, the DMFC-P would have a longer operation time than that of the DMFC fed by solution. Moreover, for DMFC-P, the water management was realized by hydrophobic CBL which could drive the cathodic water back to the anode. Therefore, the DMFC fed by pure methanol which could slowly provide sufficient reactants (methanol and water) would have a longer lifetime than the DMFC fed by the same volume of methanol solution. By the formula $W = UIt$, we can calculate the electric energy generated after a long-term operation with a certain volume of methanol. W , U , I and t represent energy, voltage, current, and duration time, respectively. Since the current is constant, product of U and t equals to the integration area between the $V-t$ curve and t -axis. The volume energy density of DMFC-P is calculated to be about 547 Wh L^{-1} . Considering the initially injected 3 mL water in cushion tank, the actual value is 438 Wh L^{-1} . The calculated energy density of 2 M solution feed DMFC is 63.4 Wh L^{-1} , far less than that of DMFC-P. The above experiment and calculation results demonstrate that the highly hydrophobic cathode backing layer played a crucial role for the long-term operation of passive DMFC-P. This could be attributed to the water back-flow effect from cathode to anode, which provided sufficient water for anodic methanol oxidation during long-term operation. As a result, the duration time and specific energy density of DMFC-P were greatly increased compared to the conventional DMFC employing methanol solution.

4. Conclusion

Cathode backing layers (CBLs) with different PTFE contents were prepared for passive air-breathing DMFC fed by pure methanol. With the same volume of fuel, the energy density of DMFC-P using the CBL with 40 wt.% PTFE was increased by six times compared to conventional DMFC (438 Wh L^{-1} vs. 63.4 Wh L^{-1}) fed by 2 M dilute solution. The optimal DMFC-P could perform a stable operation for more than 120 h. The results confirmed that highly hydrophobic CBL exhibited excellent water management which was indispensable for water back-flow effect during a long-term operation for

passive DMFC-P. It is confirmed that this study develops a practical way for the development of high-energy DMFC.

Acknowledgments

This work was supported by High Technology Research Program (863 program 2007AA05Z159, 2007AA05Z143) of Science and Technology Ministry of China, the National Natural Science Foundation of China (20876153, 20703043, 21073180, 20933004, and 21011130027) and Science & Technology Research Programs of Jilin Province (20102204).

References

- [1] X. Ren, P. Zelenay, S. Thomas, J. Davey, S. Gottesfeld, J. Power Sources 86 (2000) 111.
- [2] M. Baldauf, W. Preidel, J. Power Sources 84 (1999) 161.
- [3] C.K. Dyer, J. Power Sources 106 (2002) 31.
- [4] Q. Ye, T.S. Zhao, J. Power Sources 147 (2005) 196.
- [5] E. Peled, V. Livshits, T. Duvedevani, J. Power Sources 106 (2002) 245.
- [6] Z. Guo, Y. Cao, J. Power Sources 132 (2004) 86.
- [7] S. Eccarius, F. Krause, K. Beard, C. Agert, J. Power Sources 182 (2008) 565.
- [8] L. Feng, J. Zhang, W. Cai, Liangliang, W. Xing, C. Liu, J. Power Sources 196 (2011) 2750.
- [9] G.Q. Lu, F.Q. Liu, C.-Y. Wang, Electrochem. Solid-State Lett. 8 (2005) A1.
- [10] A. Oedegaard, C. Hebling, A. Schmitz, S. Møller-Holst, R. Tunold, J. Power Sources 127 (2004) 187.
- [11] G. Jewett, Z. Guo, A. Faghri, J. Power Sources 168 (2007) 434.
- [12] K. Nishida, T. Murakami, S. Tsushima, S. Hirai, J. Power Sources 195 (2010) 3365.
- [13] T.S. Zhao, W.W. Yang, R. Chen, Q.X. Wu, J. Power Sources 195 (2010) 3451.
- [14] Y.M. Volkovich, V.E. Sosenkin, V.S. Bagotsky, J. Power Sources 195 (2010) 5429.
- [15] J.R.M. Mathias, J. Fleming, W. Lehnert, Handbook of Fuel Cells-Fundamentals Technology and Applications, John Wiley & Sons Ltd., 2003.
- [16] Y.-H. Cho, J. Kim, M. Ahn, Y.-E. Sung, J. Power Sources 195 (2010) 5952.
- [17] F. Liu, G. Lu, C.-Y. Wang, J. Electrochem. Soc. 153 (2006) A543.
- [18] K.S.S. Naing, Y. Tabe, T. Chikahisa, J. Power Sources 196 (2011) 2584.
- [19] S.Q. Song, Z.X. Liang, W.J. Zhou, G.Q. Sun, Q. Xin, V. Stergiopoulos, P. Tsiakaras, J. Power Sources 145 (2005) 495.
- [20] M. Ali Abdelkareem, N. Nakagawa, J. Power Sources 162 (2006) 114.
- [21] T. Kitahara, T. Konomi, H. Nakajima, J. Power Sources 195 (2010) 2202.
- [22] A.P. Saab, F.H. Garzon, T.A. Zawodzinski, J. Electrochem. Soc. 150 (2003) A214.
- [23] J. Lobato, M. Rodrigo, J. Linares, J. Appl. Electrochem. 38 (2008) 793.
- [24] C. Xu, T.S. Zhao, Y.L. He, J. Power Sources 171 (2007) 268.
- [25] M. Okada, Y. Konta, N. Nakagawa, J. Power Sources 185 (2008) 711.
- [26] K.-Y. Song, H.-K. Lee, H.-T. Kim, Electrochim. Acta 53 (2007) 637.
- [27] C. Xu, T.S. Zhao, J. Power Sources 168 (2007) 143.